Design, Fabrication and Measurement of Two-Layered Quadruple-Band Microwave Metamaterial Absorber

M. R. Soheilifar, R. A. Sadeghzadeh

Faculty of Electrical and Computer Engineering, K. N. Toosi University of Technology, Tehran, Iran
rsoheilifar@ee.kntu.ac.ir, sadeghz@eetd.kntu.ac.ir
Corresponding author: M. R. Soheilifar

***Abstract*- The design, simulation, fabrication, and measurement of two structures of metamaterial absorbers (MA) is investigated at microwave frequency in this paper. By stacking of one layer structure on the top of each other, a two-layered structure is generated. The unit cell at each layer consisting of two sets of various circular and square patches are designed so that the structure exhibit quad band absorption response. The advantages of these MAs are being thin, having simple structures, excellent polarization characteristics and maintaining high absorption peaks even at large angles of incidence for both TM and TE polarizations. In addition, measurement of a fabricated prototype shows a satisfactory agreement with the respective simulation results.**

***Index Terms*- Absorber, metamaterial, multiband, microwave.**

I. INTRODUCTION

After the illustration of first perfect metamaterial absorber in spectra microwave by Landy et al.[1], metamaterial abosrbers (MA) design, fabrication, and characterization have been extensively investigated in broadband spectra that covers microwave [2, 3], terahertz [4,5], infrared [6, 7], and optical bands [8, 9]. Unfortunately, MAs' bandwidth is narrow. Although recent reports show good performance of MAs in single-band [10, 11], dual band [12, 13, 14], and triple band [15,16, 17], such as some kinds of MAs demonstrate multiple absorption peaks at variety of frequency bands, there is not enough progress in the design of multi-band (≥3 bands) MAs with high absorption.

In general, there are two kinds of assembling for structures with various geometrical parameters. The first type is the structures with various geometrical parameters which are positioned co-planar for making sure that the resonant frequencies are close to each other [18, 19, 20]. The second one is the structures with various geometrical parameters that are staked in multi-layeres [20, 21]. The efficiency of absorber can be figured out as A(ω) = 1−R(ω)−T(ω), both the transmission, T(ω), and reflection, R(ω), ought to be minimized. The background of structures are covered by a full copper plane so as to minimize T(ω). On the contrary, by minimizing reflection from the top surface of the structure, absorptivity can be maximized. It means that by matching the effective constitutive parameters of the absorber to free space, the reflection is minimized.

This paper aims at proposing a two-layered structure; ultra-thin, insensitive to polarization for a wide range of incident angles over the designed frequencies, and perfect-absorption peaks metamaterial absorbers that operate in the microwave regime. The structure of the paper is as follows. In Sec. II, the geometry of the proposed designs and angle-independent absorption characteristics are presented. To better understand the physical mechanism into the origin of the four-band absorptions, current distribution on the metals and field distribution analysis are studied. In Sec. III, the experimental setup is described. Finally, a conclusion is drawn in section V.

II. DESIGN AND SIMULATION OF UNIT CELLS

Staking structures with different geometrical parameters in multi-layered MAs [13, 22, 25] is another way for widening the bandwidth of the absorption. The side view of the proposed structure's unit cell is indicated in Fig. 1a. All circular and all square shaped unit cells are designed by means of thick FR-4 epoxy dielectric substrate ($\varepsilon_r = 4.3$, loss tanδ=0.022). The selected metal is copper with the thickness of 0.017 mm with conductivity of $\sigma = 5.96 \times 10^7$ s/m . The proposed one-layered structure consist of two sets of circular and square patches on the top of the substrate. A two-layered structure can be generated by stacking one-layered structure on the top of the other structure. The bottom of the proposed multi-layered structure's last layer is fully covered with copper. Between them, adhesive layers with the thickness of 0.06 mm are used. The MA is the periodic extension of unit cell in both x and y directions, while a plane wave which propagates along the z-axis serves as the incident radiation. Figs. 1b, 1c, and 1d demonstrate the designed structures. The sample geometric parameters are shown in Table I. Dimensions and substrate thickness are optimized in order maximum absorption takes place at microwave frequencies.

The frequency domain solver, CST Microwave Studio 2012, is used to compute reflection parameter S11. Periodic boundary conditions are employed in the x and y directions. Due to T(ω)=0, the absorption formula is in this situation. The absorption's mechanism is due to a number of cases. First, by changing the geometry of MA and the thickness of spacer, the impedance of absorber is designed to match the impedance of free space at a specific frequency; therefore, the reflection is zero [3]. Second, electromagnetic waves are not able to pass through the metallic ground plane which leads to zero transmission coefficient [3].

A. The circular MA

In this case, the MA indicates quad absorption band. For the TM mode shown in Fig. 2a, the simulation results display that the absorption peaks happen at frequencies of 9.001 GHz, 10.646 GHz, 11.388 GHz, and 12.396 GHz at normal incidence with absorption rates 95.60%, 100%, 98.80%, and
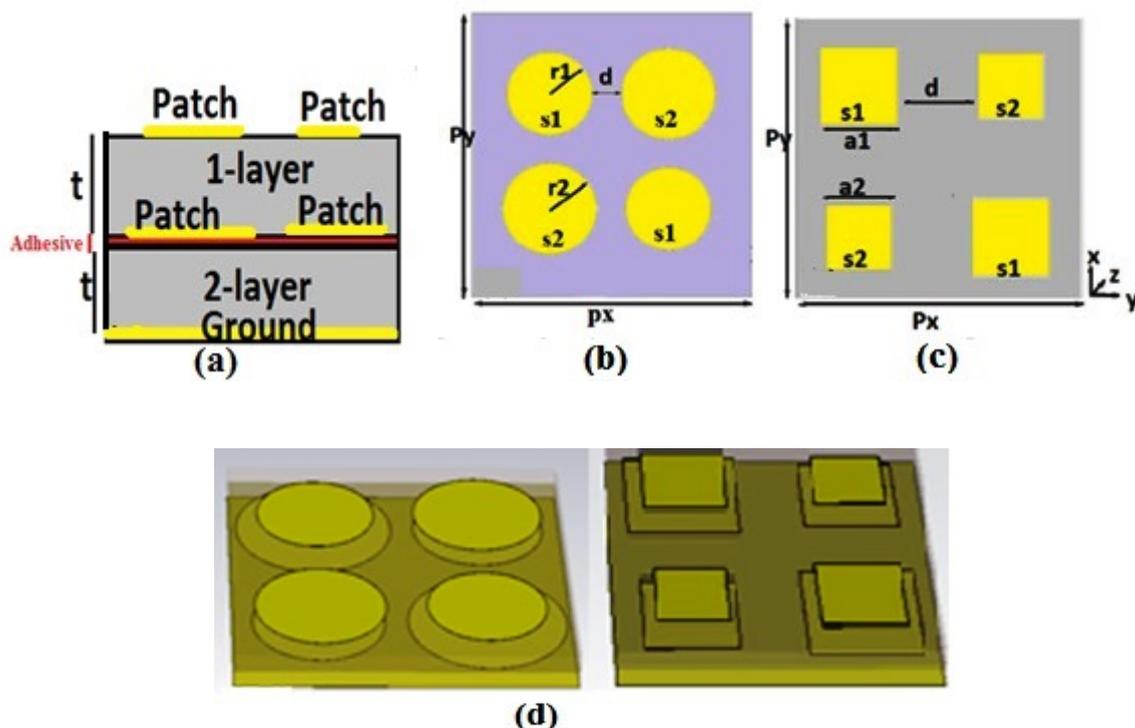
Fig. 1. Perspective view and unit cell geometry of the metamaterial absorbers (a) side view of two-layered structure, (b) top view of circular and (c) top view of square-shaped patches, (d) Simulated MAs samples.

Table. I. Dimension and substrate thickness of two-layered unit cell (unit: mm).
r1, r2, d, a1, a2: Dimension MAs, t: Substrate thicknesses, Px, Py: Periodicity

	Circular element						Square element					
Dimension	*r1*	*r2*	*d*	*Px*	*Py*	*t*	*a1*	*a2*	*d*	*Px*	*Py*	*t*
1-Layer	4.5	4.95	4.35	18.2	18.2	0.4	6.43	5.43	6.21	24.3	24.3	0.5
2-Layer	6	5	3	18.2	18.2	0.4	8.57	7.14	4.28	24.3	24.3	0.5

99.80%, respectively, and the full width at half maxima (FWHM) bandwidth is 6.742%, 6.486%, 7.449% and 4.862%, respectively.

By increasing incident angle, the four peak absorption values stay larger than 95% for all angles of oblique incidence. Having been the cause of the resonant absorption, the TM mode is capable of being effectively excited by the magnetic field that is significant to keep the impedance matching at all incident angles [14], which is depicted in Fig. 2a. In the case of TE mode, by increasing the incident angle, there will be a decrease in the absorption spectrum and a slight shift in the resonance frequency. Fig.2b demonstrates the absorption spectra in TE mode. As it is evident in TM and TE modes, there is not much alteration with angles up to θ=60°. Angle θ can be defined as the angle
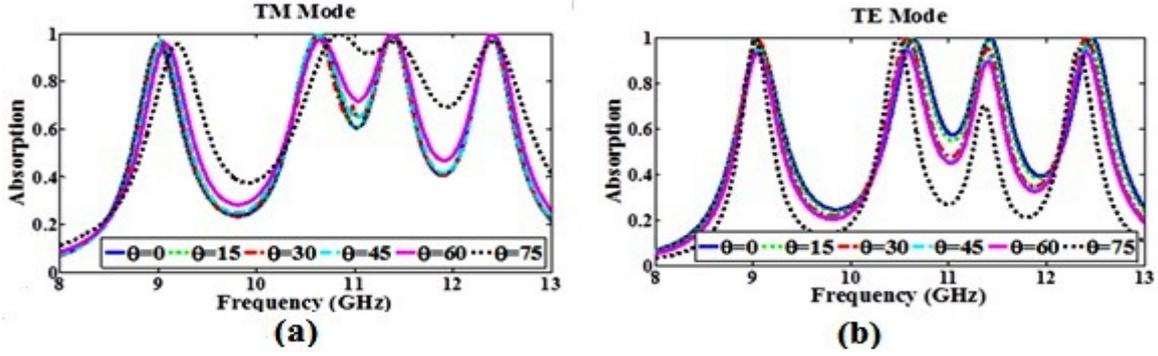
Fig. 2. The simulated results under normal and oblique incidence for two-layered circular structure, (a) TM, and (b) TE modes.

between the incident wave's propagation vector and the *z*-axis over the *yz*-plane. For both TE and TM modes, this quad-band MA operates pretty well over a large range of incident angles.

Through the use of Equation (1), the normalized input impedance is calculated. In other words, the impedance at the resonant frequency matched with free space at resonance frequencies.

$$Z = \eta_0 \sqrt{\frac{(1 + S_{11})^2 - S_{21}^2}{(1 - S_{11})^2 - S_{21}^2}}$$

(1)

For measuring or stimulating the values of S11 and S12, software such as CST can be employed. Since the bottom layer is completely covered with copper, a square with sides $c = 0.1 \times p$ (ten percent period) is eliminated from each of the four corners of the copper layer, so that the structural parameters could be calculated. It means that S12 is not equal to zero. For some *c* values, the responses of S11 have been explored. It is assessed by the researchers that the amount of eliminated corners does not have any effects on the electromagnetic waves absorption. It can be clearly seen from the curves of Fig. 4, that the Re (Z) are in close proximity to unity, while the Im (Z) are around zero for all peak absorption frequencies for supporting absorption.

B. The square MA

In square shaped, two-layered structure, four separated absorption peaks under perpendicular incidence are obtained for TM and TE polarizations. At frequency range of THz [20], researchers have reported similar structure. The first peak is at the frequency of 7.47 GHz with absorptivity of 99.5%, the second, third, and fourth resonance frequencies occur at 8.78 GHz, 10.3 GHz, and 12 GHz with absorption rates 97.4 %, 99.90%, and 98.90% and the FWHM bandwidth is 5.217%, 4.328%, 4.367% and 4.003%, respectively.

Under large angles of oblique incidence, the absorber has been explored for both TE and TM polarizations. In TM mode, when θ changes from 0° to 75°, the behavior of absorption spectrum remains roughly unchanged up to θ = 75°. That means the magnetic flux between the top layer and
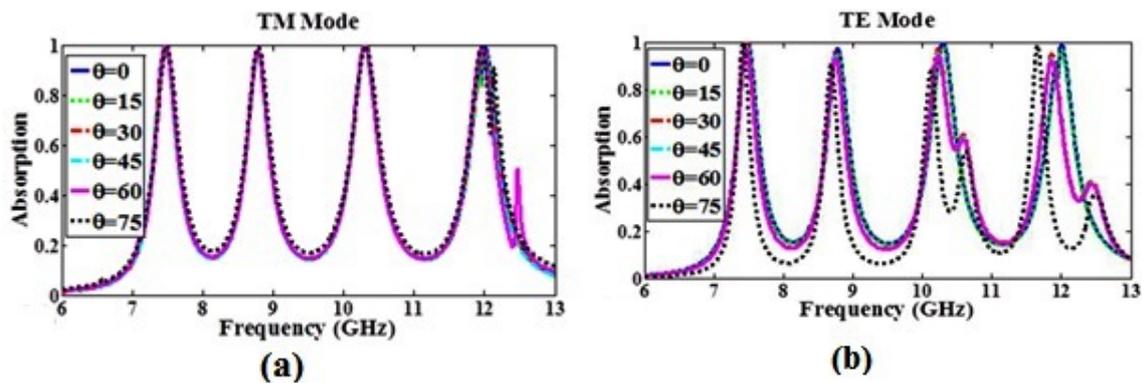
Fig. 3. The simulated results under normal and oblique incidence for two-layered square structure, (a) TM, and (b) TE modes.

bottom layer is approximately unchanged, and it can provide powerful magnetic resonance at all of the incident angles which are important to keep impedance match [24]. Regarding TE polarization, the absorption spectrum maintains nearly unchanged up to $\theta = 60°$. Over 50°, the absorptivity reduces suddenly. It is mainly due to the incident magnetic flux between the sandwiched structure that becomes less and less with the increase of incident angle [24]. Fig. 3 shows the proposed quad-band MA's simulated absorption curves for six various incident angles for both TM (Fig. 3a) and TE (Fig. 3b) modes, respectively. In addition, the impedance curves are demonstrated in Fig. 4a and Fig. 4b for TM mode. The real relative impedance is close to unity at each absorption frequency.

For better comprehension of the physical mechanism, surface current and electric field distributions obtained from simulation are studied to find out the origin of the quad-band absorptions. Due to the directions of surface current densities on the bottom layer, all absorptions in MA are in antiparallel direction with the direction of the surface current densities on the top layer. In fact, there are two accepted loss mechanisms; one is dielectric losses arising from the imaginary part of the substrate's dielectric constant and the other is ohmic losses which is because of the finite conductivity of the structure's metallic parts. In essence, it has been confirmed that their performance is principally linked with the substrate's dielectric losses [2]. The surface current distributions in different layers of the square MA's two-layered structure are shown in Fig. 5.

In Fig. 5, the distribution of the simulated electric field for the proposed MA unit cell in perpendicular incidence at frequencies of absorption is presented. It is evident that in Figs. 5a, 5e, at the lowest frequency $f1 = 7.47$ GHz, currents distribution came together in the bottom layer square plates left and right sides, bottom layer's longest metallic plate (s1 at bottom layer). Therefore, the E field is localized in the edges of the left and right sides of the bottom layer square plates (s1 at bottom layer). At $f2 = 8.78$ GHz, surface currents distribution primarily focuses on the left and right sides of the bottom layer square plates, the lowest metallic plate (s2 at bottom layer) based on Fig. 5b. As a result, as indicated in Fig. 5f, the electric field is principally restricted to those parts. In a similar way,
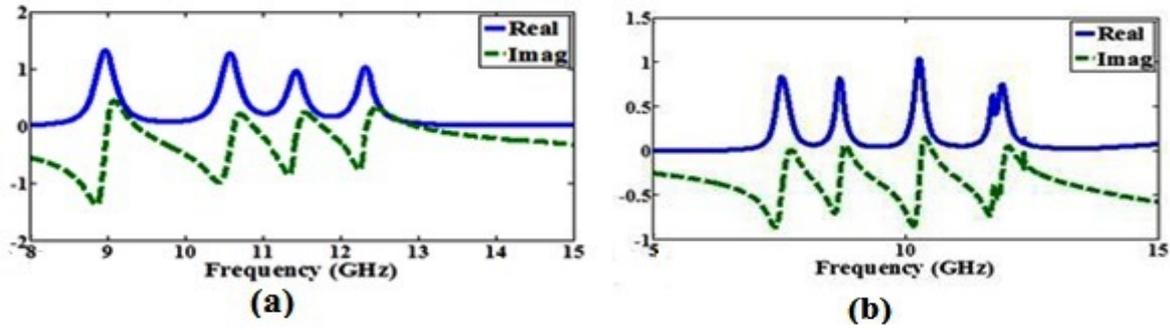
Fig. 4. Retrieved impedance result for two-layered (a) circular, and (b) square structures for TM mode

f (GHz)	Surface current			f (GHz)	Electric field		
	Top layer	Bottom layer	Ground		Top layer	Bottom layer	Ground
7.47 (a)				7.47 (e)			
8.78 (b)				8.78 (f)			
10.32 (c)				10.32 (g)			
11.99 (d)				11.99 (h)			

Fig. 5. Surface current distributions and the electric field distributions at (a), (e) f1=7.47 GHz, (b), (f) f2= 8.78 GHz, (c), (g) f3=10.32 GHz, and (d), (h) f4= 11.99 GHz.

at frequencies f3=10.32 GHz (Figs. 5c, 5g) and f4= 11.99 GHz (Figs. 5d, 5h), the distribution of current density and electric field can be described.

The results of this paper are almost identical with some previously reported results with quad-band resonance structures. In Table II, the results are compared with each other.

III. FABRICATION AND CHARACTERIZATION

The sample structures, designed in the previous section, are fabricated and measured with dimension of 309.4 mm ×309.4 mm (for circular unit cells) and 291.6 mm × 291.6 mm (for square unit cells). We have used a vector network analyzer (Agilent E8362) and two X-band microwave rectangular horn antennas. The horn antennas have a voltage standing wave ration (VSWR) of <2 over a wide frequency range from 1 to 18 GHz. Before starting the characterization measurements, we

Table. II. Comparing the results of this paper and some other MAs reported previously, quad band

ID	Thickness (mm)	Frequency (GHz)	Absorption %	FWHM %	Design	Wide-Angle range
Ref. 13/ [2013]	1	5.22 7.44 9.96 10.48	97.10 91.30 98.30 90.70	5.00 6.00 The last two 9.00	Complex	0° to 45°
Ref. 26/ [2015]	0.217	28.21 35.59 52.78 53.63	99.47 99.94 99.15 99.55	-	Easy	0° to 40°
Ref. 27/ [2014]	1	6.16 8.76 11.32 12.54	99.98 99.89 42 99.82	3.00 4.00 0 4.00	Complex	0° to 60°
Ref 28/ [2015]	1	3.91 5.16 7.10 9.16	99.35 98.04 99.85 99.78	2.00 2.00 3.00 3.50	Easy	0° to 45°
This paper (Circular MA)	0.8	9.001 10.646 11.388 12.396	95.60 100.00 98.80 99.80	6.74 6.48 7.44 4.86	Very easy	0° to 60°
This paper (Square MA)	1	7.470 8.780 10.300 12.000	99.50 97.40 99.90 98.90	5.21 4.32 4.36 4.00	Very easy	0° to 60°

have performed a through-reflect-line calibration. The reference plane is located at the surface of the sample. The reflection measurement has been calibrated by replacing the sample with an aluminium plat of same size at reference plane. The transmission measurement has been calibrated with no sample.

Measurements are studied for both linear polarizations under normal and oblique incidence. The noise of anechoic chamber is measured in the absence of any samples. The noise stays roughly below -30 dB in the total frequency range. In this measurement, the most important error sources are due to the fabrication tolerance and restrictions in the precise measurement of coefficient S11.

To obtain the $S11$ parameters, two horns are focused on the sample sheet on the same side, as shown in Fig. 6(d). The height of the horn antennas (which are 120 mm wide and 90 mm long) is maintained at 1.2 m and the distance between horns and sample sheet is 6 m to eliminate near field coupling effects of the horn antenna to minimize the effect of near-field as well as diffraction. The structure is kept at a distance much larger than $2D^2/\lambda$, where D is the maximum dimension.

All samples which are measured are taken in the following respect. First, in each step, position transmitter antenna is turned 15 degrees. The transmitter and receiver antennas are both on one side of the samples. Second, both linear polarizations could be measured by rotating the antennas with the horizontal z axis. Third, bottom layer is completely covered with copper. As a result, we can define the absorption as $A(\omega) = 1 - R(\omega)$, that $R(\omega) = |S11|^2$. Therefore, only S11 coefficient's measurement is
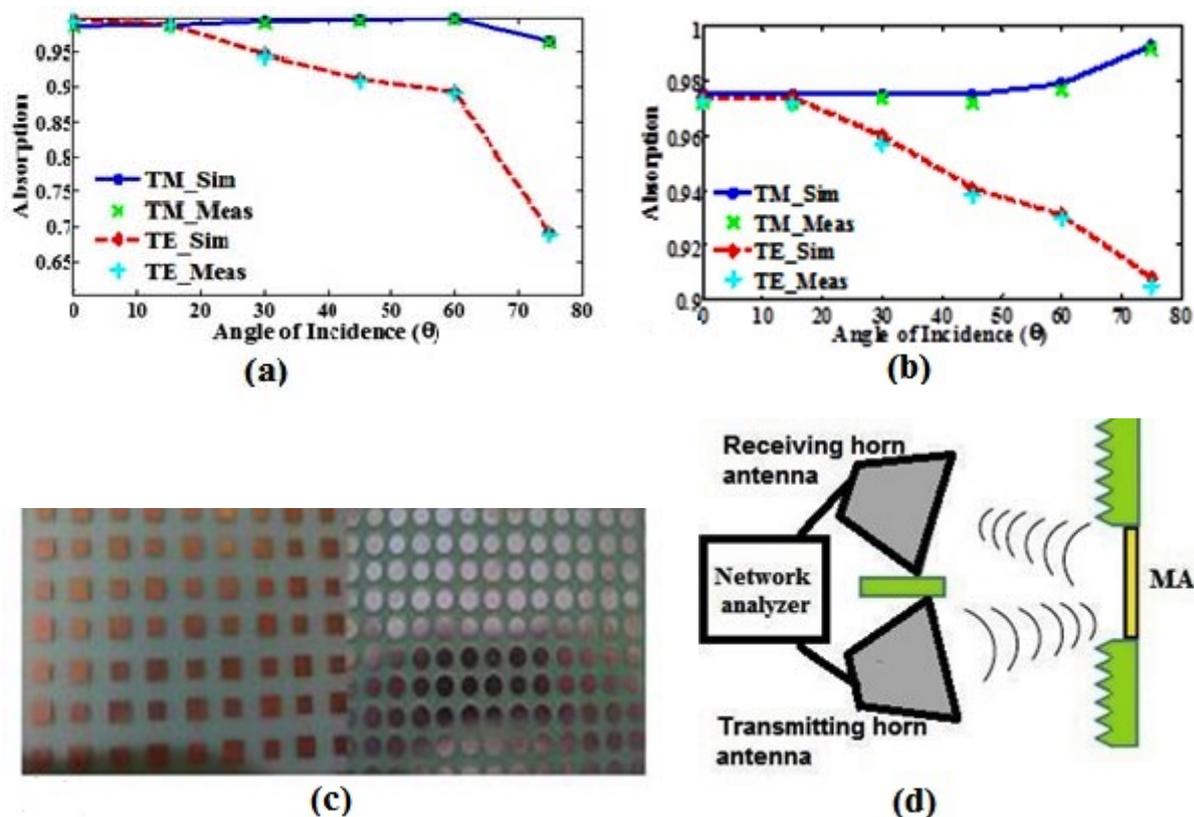
Fig. 6. The comparison of simulated and measured results for the TM and TE modes under normal and oblique incidence, (a) the two-layered structure with circular cells, (b) the two-layered structure with square cells. (c) Fabricated metamaterial absorber, (d) The experimental setup in which the MA sample is placed in the center of flat base.

needed. Prototype metamaterial absorbers are fabricated with a stacking of two-layered for experimentation.

Measurements are made at the resonant frequency of 11.388 GHz for a two-layered structure which includes circular patches. Fig. 6a demonstrates the comparison of the absorption spectrum with measured and simulated. It can be seen that a good agreement exists between simulation and measurements. As displayed in Fig. 6b, in a two-layered MA with square patches for both TM and TE modes, the measured and simulated results fit well up to θ=75°. In such a case, simulations results and those measurements are in a good agreement. Measurements are taken at the resonant frequency of 8.780 GHz. Fig. 6c is the portion of the photograph of the top layer circular and square metamaterial absorber.

Fig. 7a and Fig. 7b shows the measured absorptive spectrum for TM mode and under normal incidence wave. Through the comparison, we can observe that the simulations results are in good agreement with experiments for the two-layered structure with circular cells. In addition, the two-layered structure with square cells, there is also a slight frequency shift in the range of 185 MHz for all the peaks. The slight frequency discrepancy may be due to the tolerances that are inherent in the
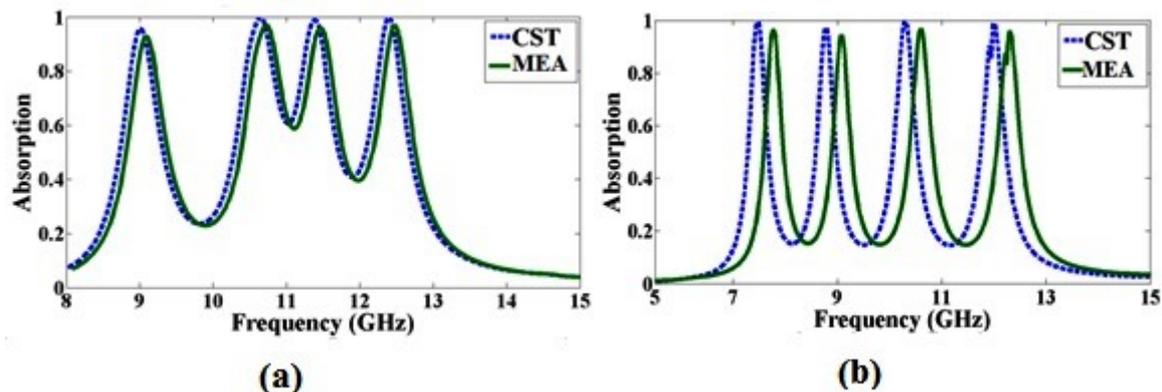
Fig. 7. Simulated (blue curve) and measured (green curve) absorption spectra of the quad-band MA under normal incidence (TM incidence), for the two-layered (a) circular, and (b) square structures.

fabrication process. Also, experimental conditions can induce discrepancies such as background interference. The absorption measurement is 1.2% lower than simulation results.

IV. CONCLUSION

In conclusion, the designed and fabricated two-layered metamaterial abosober is investigated. Each layer is the combination of two sets of different geometric dimensions including circular and square metallic plates. In circular and square MAs in both TE and TM cases, it is evident that there are four close to unity absorption peaks approximately for all of the angles of oblique incidence (from 0° to 60°). In all MAs, it is seen that the experimental results and simulations are in good agreement.

REFERENCES

[1] N. I. Landy, S. Sajuyigbe, J. Mock, D. R Smith, and W. J. Padilla, "Perfect metamaterial absorber," Phys. Rev. Lett., vol. 100, pp. 207402- 207406, 2008.

[2] A. Dimitriadis, N. Kantartzis, and T. Tsiboukis, "A polarization-/angle-insensitive, bandwidth- optimized, metamaterial absorber in the microwave regime," Appl. Phys. A., vol. 109, pp. 1065–1070, 2012

[3] M. R. Soheilifar, R. A. Sadeghzadeh,"Design, simulation and fabrication of an ultra-thin planar microwave metamaterial absorber," Microwave Opt Technol Lett, vol. 56, pp. 2916- 2922, 2014.

[4] B. X. Wang, L. L. Wang, G. Z. Wang, L. Wang, X. Zhai, X. F. Li, W. Q. Huang, "A simple nested metamaterial structure with enhanced bandwidth performance," Opt Commun., vol. 303, pp. 13–14, 2013.

[5] B. X. Wang, L. Wang, G. Z. Wang, "Theoretical investigation of broadband and wide-angle terahertz metamaterial absorber," IEEE Photonics Technology Letters., vol. 26, pp. 111-114, 2014.

[6] L. Meng, D. Zhao, Q. Li, and M. Qiu, "Polarization-sensitive perfect absorbers at near-infrared wavelengths," Opt Express, vol. 21, pp. A229-A230, 2013.

[7] W.R. Zhu, W. R., X. P. Zhao, B. Y. Gong, L. H. Liu, and B. Su, "Optical metamaterial absorber based on leaf- shaped cells," Appl. Phys. A., vol. 102, pp. 147-151, 2011.

[8] C. G. Hu, Z. Y. Zhao, X. N. Chen, and X. G. Luo, "Realizing near-perfect absorption at visible frequencies," Opt Express, vol. 17, pp. 11039-11044, 2009.

[9] J. Ng, H.Y. Chen, and C.T. Chan, "Metamaterial frequency-selective super absorber," Opt Lett., vol. 34, pp. 644-646, 2009.

[10] L. H. Huang, D. R. Chowdhury, S. Ramani, M. T. Reiten, S. N. Luo, A. K. Azad, A. J. Taylor, and H. T. Chen, "Impact of resonator geometry and its coupling with ground plane on ultrathin metamaterial perfect absorbers," Appl Phys Lett., vol. 101, pp. 101102-101108, 2012.

[11] Y. Cheng, H. Yang, Z. Cheng, N. Wu, "Perfect metamaterial absorber based on a split-ring-cross resonator,"Appl Phys A., vol 102, pp. 99-103, 2011.

[12] B. Ni, X. S. Chen, L. J. Huang, J. Y. Ding, G. H. Li, W.A. Lu, "Dual band polarization insensitive metamaterial absorber with split ring resonator," Opt Quant Electron, vol. 45, pp. 747-753, 2013.

[13] Y. Cheng, Y. Nie, and R. Gong, "Metamaterial absorber and extending absorbance bandwidth bsed on multi- cross resonators," Appl Phys B., vol. 111, pp. 483-488, 2013.

[14] J. Zhong, Y. Huang, G. Wen, H. Sun, P. Wang, and O. Gordon, "Single-/dual-band metamaterial absorber based on cross-circular-loop resonator with shorted stubs," Appl Phys A., vol 108, pp. 329-335, 2012.

[15] B. Somak, G. Saptarshi, and V.S. Kumar," Triple band polarization-independent metamaterial absorber with bandwidth enhancement at X-band," J Appl Phys., vol. 114, pp. 094514-1-094514-7, 2013.

[16] B. Bian, L. Liu, S. Wang, X. Kong, H. Zhang, B. Ma, and H. Yang, "Novel triple-band polarization-insensitive wide-angle ultra-thin microwave metamaterial absorber," J Appl Phys., vol. 114, pp. 194511-1-194511-6, 2013.

[17] Y. Qiwei, L. Ying, L. Hai, L. Minhua, and Y. Helin, "Multi-band metamaterial absorber made of multi-gap SRRs structure," Appl Phys A., vol 107, pp. 155-160, 2012.

[18] M. R. Soheilifar, R.A. Sadeghzadeh, and H. Gobadi,"Design and fabrication of a metamaterial absorber in the microwave range," Microwave Opt Technol Lett., vol. 56, pp. 1748-1752, 2014.

[19] T. M. Kollatou, A. I. Dimitriadis, S. D. Assimonis, N. V. Kantartzis, C. S. Antonopoulos, "Multi-band, highly absorbing, microwave metamaterial structures," Appl. Phys. A., vol. 115, pp. 555-561, 2014.

[20] M. R. Soheilifar, R. A. Sadeghzadeh, "Design, fabrication and characterization of scaled and stacked layers planar metamaterial absorber, " IET Microwave, Antennas & Propagation, vol. 9, pp. 86-93, 2015.

[21] B. X. Wang, L. L. Wang, G. Z. Wang , W. Q. Huang, X. F. Li, X. Zhai, "A simple design of ultra-broadband and polarization insensitive terahertz metamaterial absorber," Appl. Phys. A., vol. 115, pp. 1187-1192, 2013.

[22] B.X. Wang, L. L. Wang, G. Z. Wang, W. Q. Huang, X. F. Li, X. Zhai, "Metamaterial-based low-conductivity alloy perfect absorber," Appl. Journal of Light Wave Technology, vol. 32, pp. 2293-2298, 2014.

[23] C. G. Hu, X. Li, Q. Feng, X. Chen, and X. Luo, "Investigation on the role of the dielectric loss in metamaterial absorber," Opt. Express, vol. 18, pp. 6598-6603, 2010.

[24] W. R. Zhu, and X.P. Zhao, "Metamaterial absorber with dendritic cells at infrared frequencies," J. Opt. Soc. Am. B., vol. 26, pp. 2382-2385, 2009.

[25] M. R. Soheilifar, R. A. Sadeghzadeh,"Design, fabrication and characterization of stacked layers planar broadband metamaterial absorber at microwave frequency," AEUE Int. J. Electron. Commun (Elsevier). vol. 69, pp. 126-132, 2015.

[26] N.Wang, J . Tong, W. Zhou, W. Jiang, J. Li, X. Dong, S. Hu," Novel quadruple-band microwave metamaterial absorber," Photonics Journal, IEEE, vol. 7, 2015.

[27] B. Ma, S. Liu, B. Bian, X. Kong, H. Zhang, Z. Mao, and B.Wang, " Novel three-band microwave metamaterial absorber," Journal of Electromagnetic Waves and Applications, vol. 28, pp. 1478- 1486, 2014.

[28] D. Chaurasiya, et. al."An ultrathin quad- band polarization- insensitive wide- angle metamaterial absorber," Microwave Opt Technol Lett., vol. 55, pp. 697- 702, 2015.